ENERGY TRANSPORT IN SEMICONDUCTOR DEVICES

ANSGAR JÜNGEL

ABSTRACT. The modeling, analysis, and numerical approximation of energy-transport models for semiconductor devices is reviewed. The derivation of the partial differential equations from the semiconductor Boltzmann equation is sketched. Furthermore, the main ideas for the analytical treatment of the equations, employing thermodynamic principles, are given. A new result is the proof of the weak sequential stability of approximate solutions to some time-dependent energy-transport equations with physical transport coefficients. The discretization of the stationary model using mixed finite elements is explained, and some numerical results in two and three space dimensions are presented. Finally, energy-transport models with lattice heating or quantum corrections are discussed.

1. INTRODUCTION

The transport of charge carriers in semiconductors has to be described on the most basic level in a quantum mechanical way. The large number of electrons, however, makes it necessary to follow a statistical approach using a probability distribution and to incorporate the quantum mechanical effects semi-classically. The distribution function may be determined as the solution of a kinetic equation such as the Boltzmann equation. It contains much more information about the state of the system than actually needed. The variables of interest are typically the carrier density, mean velocity, and energy, which are averaged quantities of the probability distribution over the momentum space (so-called moments). Moreover, the direct solution of the Boltzmann equation is very time-consuming even with modern computers. Therefore, one aims to derive simpler model equations which still contain the most important physical information.

When collisions are dominant in the semiconductor domain, the ratio between the particle mean free path and the reference length (the so-called Knudsen number) is very small, and the distribution function may be expanded in the Knudsen number. This leads in the Chapman-Enskog approach to diffusive evolution equations for the moments. The lowest-order equation, the drift-diffusion equation, describes the evolution of the particle density only. Although this model gives very fast and satisfactory simulation results for semiconductor devices on the micrometer scale, it is not able to cope with so-called hot-electron effects in nanoscale devices. A possible solution is to incorporate the mean energy in the model equations, leading to energy-transport equations, which describe the evolution of

2000 *Mathematics Subject Classification.* 35K55, 35J60, 65L60, 65M60, 82D37.

Key words and phrases. Energy-transport equations, semiconductors, existence analysis, weak sequential stability, finite-element approximation..

the particle density and energy. The advantage of these models is that they have a nice mathematical structure which helps to devise efficient numerical schemes.

In this survey, we sketch the derivation of the energy-transport models from the semiconductor Boltzmann equation, review the thermodynamic structure of the model equations, summarize the existence analysis, and explain the numerical techniques used to solve them.

The first energy-transport model has been presented by Stratton in 1962 [79]. His approach is based on the relaxation time approximation of the collision integral to obtain an approximate explicit solution for the distribution function. Since then, energy-transport models have been widely used for numerical computations mostly with phenomenological transport coefficients [7, 49, 74, 77]. In the engineering literature, the energy-transport model is often considered as an approximation of the hydrodynamic equations by (essentially) neglecting convection [7, 73]. There exist many versions of the energy-transport equations, also called *energy-balance models*, derived under various hypotheses on the scattering terms, the semiconductor band structure, and the degeneracy, see e.g. [20, 39, 77, 83]. A more rigorous derivation from a diffusion approximation of the Boltzmann equation has been first presented in [11], later improved and extended in [10, 31, 32]. Energy-transport models derived from a high-field limit [34] or involving impact ionization [27] have been studied too.

Mathematicians started to pay attention to energy-transport models in the 1990s, in particular for numerical discretizations, using finite-difference methods [40, 71, 72], (mixed) finite-volume techniques [12, 18, 19], and (mixed) finite-element schemes [24, 31, 41, 51, 52, 62, 68]. Less standard techniques are essentially nonoscillatory (ENO) schemes [53], exponential difference methods [69], and pseudo-hyperbolic schemes [80]. On the other hand, there are only a few analytical results, mainly due to the strong nonlinear coupling in the equations. In earlier works, the drift-diffusion equations with temperature-dependent mobilities but without temperature gradients [84] (also see [48]) or with nonisothermal systems containing simplified thermodynamic forces [5] have been studied. Later, existence results for the complete energy-transport equations have been achieved, see [37, 46] for stationary solutions near thermal equilibrium, [21, 22, 23] for transient solutions close to equilibrium, and [29, 30] for systems with nondegenerate diffusion coefficients. Furthermore, the nonlinear stability of classical bounded solutions to the one-dimensional equations was investigated [4]. All these results give only partial answers to the well-posedness problem, and a complete global existence result for any data and with physical transport coefficients is still missing.

The review is organized as follows. In Section 2, we introduce the semiconductor Boltzmann equation, explain the main collision mechanisms, and sketch, following [32], the derivation of the energy-transport models. Furthermore, relations to nonequilibrium thermodynamics are highlighted, and explicit models are computed. Section 3 is devoted to the mathematical analysis of the time-dependent equations. We explain how the thermodynamic (entropy) structure can be employed to deduce a priori estimates, and we prove the weak sequential stability of certain approximate solutions. This proof is presented here for the first time. In Section 4, the main ideas of the discretization with mixed finite elements are introduced, and some numerical simulations of field-effect transistors in two and three

space dimensions, taken from [41, 52], are given. Finally, we mention in Section 5 some actual research directions.

2. Derivation of the model equations

2.1. **Boltzmann transport equation.** Before we detail the derivation of the model, we introduce shortly in some basic notions of semiconductor theory. For details about semiconductor physics, we refer to the textbooks [8, 13, 64]. A semiconductor crystal is modeled as a three-dimensional array of atoms arranged in a lattice. The quantum states of the electrons in the periodic lattice are given by the eigenfunctions $\psi_n(k)$, $n \in \mathbb{N}$, of a suitable Schrödinger equation, indexed by the so-called pseudo-wave vector $k \in B$, where the subset $B \subset \mathbb{R}^3$ is the Brillouin zone [55, 67]. The corresponding eigenvalue $E(k) = E_n(k)$ represents the energy of the state k in the n-th band. According to Pauli's exclusion principle, no two electrons may occupy the same quantum state simultaneously.

Instead of a full quantum description, we prefer a semi-classical approach in which the electrons in the conduction band of the semiconductor are modeled statistically and quantum effects enter only through the band structure $E(k)$. Let $f(x,k,t)$, with the spatial variable $x \in \mathbb{R}^3$ and the time $t > 0$, be the ratio of the number of occupied quantum states of the electrons in the infinitesimal volume element $dx\,dk$ in the conduction band to the total number of states in $dx\,dk$ in the conduction band. By Liouville's theorem, the distribution function $f(x,k,t)$ is constant along the particle trajectories. Then, differentiation along the trajectories gives the scaled semiconductor Boltzmann transport equation

$$\alpha^2\partial_t f_\alpha + \alpha\big(v(k)\cdot\nabla_x f_\alpha + \nabla_x V\cdot\nabla_k f_\alpha\big) = Q(f_\alpha), \quad x\in\mathbb{R}^3,\ k\in B,\ t>0, \tag{1}$$

where $\alpha > 0$ is the Knudsen number (or scaled mean free path), $v(k) = \nabla_k E(k)$ the electron group velocity, and $Q(f)$ the collision operator. We consider physical regimes in which scattering dominates transport, i.e. $\alpha \ll 1$. The Boltzmann equation is complemented with periodic boundary conditions for $k \in B$ and initial conditions for f at $t = 0$. The electric potential V may by a given function or selfconsistently defined by the Poisson equation

$$\lambda^2\Delta V = \int_B f dk - C(x),$$

where λ denotes the (scaled) Debye length and $C(x)$ models fixed charged background ions in the semiconductor crystal (doping profile).

The collision operator is assumed to be the sum of elastic, electron-electron, and inelastic scattering terms,

$$Q(f) = Q_{\rm el}(f) + \alpha Q_{\rm ee}(f) + \alpha^2 Q_{\rm in}(f).$$

In this formulation, elastic collisions dominate, and inelastic scattering is of the order $O(\alpha^2)$ only. The elastic collision operator may be given by

$$(Q_{\rm el}(f))(x,k,t) = \int_B \sigma(x,k',k)\delta(E(k') - E(k))(f' - f)dk', \tag{2}$$

which models acoustic phonon scattering in the elastic approximation, for instance. In the above integral, σ is a scattering rate, δ is the Dirac distribution, and $f' = f(x,k',t)$.

The integral can be defined more precisely by means of the coarea formula [55, Chap. 4]. Binary carrier-carrier scattering may be described by

$$(Q_{\rm ee}(f))(x,k,t) = \int_{B^3} s(x,k',k,k_1',k_1) \\ \times \big(f'f_1'(1-f)(1-f_1) - ff_1(1-f')(1-f_1')\big)dk'\,dk_1\,dk_1',$$

where the transition rate reads as

$$s(x,k',k,k_1',k_1) = \sigma(x,k',k,k_1',k_1)\delta\big(E(k')+E(k_1')-E(k)-E(k_1)\big),$$

and we employed the abbreviation $f_1 = f(x,k_1,t)$ etc. More precisely, the delta distribution should be understood as B-periodic in order to account for so-called umklapp processes (which preserve the periodic structure in k). Finally, inelastic scattering may be modeled by the integral

$$(Q_{\rm in}(f))(x,k,t) = \int_B \big(s(x,k',k)f'(1-f) - s(x,k,k')f(1-f')\big)dk'.$$

In the case of inelastic phonon scattering, the transition rate $s(x,k',k)$ is given by

$$s(x,k',k) = \sigma(x,k',k)\big((1+N)\delta(E(k')-E(k)+E_{\rm ph}) + N\delta(E(k')-E(k)-E_{\rm ph})\big),$$

where N is the phonon occupation number, and the delta distributions contribute only if a phonon with wave energy $E_{\rm ph}$ is absorbed or emitted, i.e. $E(k') = E(k) \pm E_{\rm ph}$.

We need the following properties of the above collision operators [55]. All three operators conserve mass,

$$\int_B Q_{\rm el}(f)dk = \int_B Q_{\rm ee}(f)dk = \int_B Q_{\rm in}(f)dk = 0,$$

and the elastic scattering operator conserves additionally energy,

$$\int_B Q_{\rm el}(f)E(k)dk = 0.$$

The kernel of the linear elastic scattering integral (2) consists of functions which depend only on the energy, i.e. $Q_{\rm el}(f) = 0$ if and only if $f(x,k,t) = F(x,E(k),t)$ for some functions F. Furthermore, $Q_{\rm ee}(f) = 0$ holds for Fermi-Dirac distributions, $f = (1+\exp((E(k)-\mu)/T))^{-1}$, where the chemical potential μ and the electron temperature $T > 0$ are some parameters.

2.2. **Chapman-Enskog expansion.** The main idea of the derivation of the energy-transport equations is to multiply the Boltzmann equation (1) by the weights 1 and $E(k)$ and to integrate the resulting equations over the wave-vector space, leading to the moment equations

$$\partial_t \int_B f_\alpha dk + \frac{1}{\alpha}{\rm div}_x \int_B f_\alpha v dk = 0, \tag{3}$$

$$\partial_t \int_B f_\alpha E dk + \frac{1}{\alpha}{\rm div}_x \int_B f_\alpha v E dk + \frac{1}{\alpha}\int_B \nabla_x V\cdot\nabla_k f_\alpha E dk = \frac{1}{\alpha^2}\int_B Q(f_\alpha)E dk. \tag{4}$$

The integrals $\int_B f_\alpha dk$ and $\int_B f_\alpha E dk$ can be interpreted as the particle and the energy densities, respectively, and the integrals over $f_\alpha v$ and $f_\alpha vE$ are the particle and energy fluxes, respectively.

In order to derive constitutive relations for the fluxes, we assume that the Knudsen number α is very small and expand the distribution function f_α in α. The derivation follows the lines of [32]. First, we let formally $\alpha \to 0$ in the Boltzmann equation (1), leading to $Q_{\rm el}(f) = 0$, where $f = \lim_{\alpha\to 0} f_\alpha$. Then, by assumption, $f(x,k,t)$ depends only on the energy $E(k)$, $f(x,k,t) = F(x,E(k),t)$ for some function F. Second, we introduce the Chapman-Enskog expansion $f_\alpha = F + \alpha g_\alpha$ (which defines in fact g_α), insert this expression in (1), and let $\alpha \to 0$:

$$Q_{\rm el}(g) = v(k)\cdot\nabla_x F + \nabla_x V\cdot\nabla_k F - Q_{\rm ee}(F), \tag{5}$$

where $g = \lim_{\alpha\to 0} g_\alpha$. The most difficult part now is to solve this operator equation. It can be shown that (5) is (formally) solvable if and only its integral over the energy surface of energy ε vanishes [55]:

$$\int_B Q_{\rm ee}(F)\delta(E(k)-\varepsilon)dk = 0 \quad \text{for all } \varepsilon\in\mathbb{R}.$$

This implies that F is a Fermi-Dirac distribution, $F = F_{\mu,T} = (1+\exp((E(k)-\mu)/T))^{-1}$ for some functions $\mu = \mu(x,t)$ and $T = T(x,t)$. Since $Q_{\rm ee}(F_{\mu,T}) = 0$, we infer from (5) that

$$Q_{\rm el}(g) = v(k)\cdot\nabla_x F + \nabla_x V\cdot\nabla_k F. \tag{6}$$

Integrating this equation and observing that $Q_{\rm el}$ conserves mass and energy, we find that

$$0 = \int_B v\cdot\nabla_x F dk = \int_B \big(v\cdot\nabla_x F + \nabla_x V\cdot\nabla_k F\big)E dk. \tag{7}$$

Third, we insert the Chapman-Enkog expansion into the moment equations (3)-(4):

$$\begin{aligned}
&\partial_t\int_B F dk + \frac{1}{\alpha}\int_B v\cdot\nabla_x F dk + \int_B v\cdot\nabla_x g_\alpha dk = O(\alpha),\\
&\partial_t\int_B FE dk + \frac{1}{\alpha}\int_B \big(v\cdot\nabla_x F + \nabla_x V\cdot\nabla_k F\big)E dk\\
&\qquad + \int_B \big(v\cdot\nabla_x g_\alpha + \nabla_x V\cdot\nabla_k g_\alpha\big)E dk = \int_B Q_{\rm in}(f_\alpha)E dk + O(\alpha),
\end{aligned}$$

where we have used that the elastic and electron-electron collisions conserve mass and energy and that the inelastic collisions conserve mass. Because of (7), the integrals of order α^{-1} vanish, and we obtain in the limit $\alpha\to 0$:

$$\partial_t n - \mathrm{div}_x J_n = 0, \quad \partial_t(ne) - \mathrm{div}_x J_e + J_n\cdot\nabla_x V = W, \tag{8}$$

where the particle and energy densities n and ne and the particle and energy current densities J_n and J_e are defined by

$$n = \int_B F dk, \quad ne = \int_B FE dk, \quad J_n = -\int_B gv dk, \quad J_e = -\int_B gvE dk, \tag{9}$$

and $W = \int_B Q_{\rm in}(F)Edk$ describes averaged inelastic scattering. Notice that we have integrated by parts in the energy equation and employed the definition of the velocity $v = \nabla_k E$.

It remains to derive expressions for the current densities which depend on n and ne. To this end, we introduce the vector-valued solution d_0 of $Q_{\rm el}(d_0) = -vF(1-F)$. It can be shown that this solution exists. In view of (6), we can decompose $g = -d_0 \cdot (\nabla_x(\mu/T) - \nabla_x V/T - E\nabla_x(1/T)) + F_1$, where F_1 is some element of the kernel of $Q_{\rm el}$. This implies that

$$J_n = D_{00}\left(\nabla_x\Big(\frac{\mu}{T}\Big) - \frac{\nabla_x V}{T}\right) - D_{01}\nabla_x\Big(\frac{1}{T}\Big), \tag{10}$$

$$J_e = D_{10}\left(\nabla_x\Big(\frac{\mu}{T}\Big) - \frac{\nabla_x V}{T}\right) - D_{11}\nabla_x\Big(\frac{1}{T}\Big), \tag{11}$$

and the diffusion coefficients D_{ij} are defined by

$$D_{ij} = D_{ij}(\mu,T) = \int_B E^{i+j} v \otimes d_0 dk, \quad i,j = 0,1. \tag{12}$$

Equations (8) and (10)-(12) are referred to as the *energy-transport equations*. They are complemented by initial conditions for n and T and, in bounded domains, by mixed Dirichlet-Neumann boundary conditions for n and T. Notice that the densities (n, ne) are functions of (μ, T) through (9) and $F = F_{\mu,T}$. Equations (8) can be interpreted as balance equations of mass and energy, and (10)-(11) are the constitutive equations for the particle and heat fluxes. Under a weak condition on the band structure, it is shown in [11] that the diffusion matrix (D_{ij}) is symmetric and positive definite.

2.3. **Thermodynamic structure of the equations.** In nonequilibrium thermodynamics, the formulation of the energy-transport model (8), (10)-(11) is well known. Indeed, the thermodynamic fluxes depend linearly on the thermodynamic forces $X_0 = \nabla(\mu/T) - \nabla V/T$ and $X_1 = -\nabla(1/T)$ [47]. The variables $u_0 = \mu/T$ and $u_1 = -1/T$ are known as the (primal) entropy variables. The connection to thermodynamics has two important consequences. First, by introducing the dual entropy variables $w_0 = (\mu - V)/T$ and $w_1 = -1/T$, the current densities can be written in the "symmetric" form

$$\widetilde{J}_n = \sum_{i=0}^1 L_{0i}\nabla w_i, \quad \widetilde{J}_e = \sum_{i=0}^1 L_{1i}\nabla w_i, \tag{13}$$

where $L_{00} = D_{00}$, $L_{01} = L_{10} = D_{01} - D_{00}V$ and $L_{11} = D_{11} - 2D_{01}V + D_{00}V^2$, and the balance equations become

$$\partial_t n - \mathrm{div}\widetilde{J}_n = 0, \quad \partial_t(ne - nV) - \mathrm{div}\widetilde{J}_e = W. \tag{14}$$

The dual entropy variables have "symmetrized" the model in the sense that the convective terms $J_n \cdot \nabla V$ in (8) and $D_{i0}\nabla V/T$ in (10)-(11) are eliminated. As we will explain below, this simplifies the mathematical analysis and it is useful for designing numerical approximations.

Second, the existence of a symmetrizing change of unknowns implies the existence of an entropy (or free energy) functional. Let us consider the whole-space situation (the case of bounded domains is treated in Section 3.1). The entropy reads as

$$S(u) = \int_{\mathbb{R}^3} s(u)dx = \int_{\mathbb{R}^3} \big(\rho \cdot u - \chi(u)\big)dx,$$

where $\nabla_u \chi(u) = \rho(u)$, and the entropy density s relates the extensive variables $\rho = (n, ne)$ and the intensive variables $u = (u_0, u_1)$ through $u = \partial s/\partial\rho$. In fact, the entropy density s can be interpreted as the Legendre transform of χ. Differentiating S formally with respect to t and assuming that the potential is time-independent, we compute

$$\frac{dS}{dt} = \int_{\mathbb{R}^3} \partial_t \rho \cdot u dx = -\sum_{i,j=0}^{1} \int_{\mathbb{R}^3} L_{ij} \nabla w_i \cdot \nabla w_j dx + \int_{\mathbb{R}^3} W u_1 dx.$$

Since the diffusion matrix (D_{ij}) is symmetric and positive definite (under weak conditions on the band structure), so is (L_{ij}), and we find that

$$\frac{dS}{dt} + c\int_{\mathbb{R}^3} |\nabla w|^2 dx \le \int_{\mathbb{R}^3} W u_1 dx, \tag{15}$$

where $c > 0$. Neglecting the source term W, S is a nonincreasing function in t. This property is extremely useful to derive a priori estimates for the solutions and to study their long-time behavior.

2.4. **Explicit models.** The formulation (8), (10)-(12) is not explicit in the macroscopic variables (n, ne) or (μ, T). Explicit expressions are obtained under simplifying assumptions. We assume that the semiconductor material is nondegenerate such that the Fermi-Dirac distribution F in (9) can be approximated by the Maxwellian $\exp(-(E-\mu)/T)$, that the energy band is given by the parabolic approximation $E(k) = |k|^2/2$, $k \in \mathbb{R}^3$, and that the elastic scattering rate σ in (2) is proportional to E^β with $\beta \ge 0$ (see [64, Sec. 2.3.4]). Finally, we suppose that the averaged inelastic collision integral W is approximated by a Fokker-Planck ansatz [31]. Then the extensive variables can be formulated as

$$n = N_0 T^{3/2} e^{\mu/T}, \quad ne = \frac{3}{2} nT,$$

where $N_0 T^{3/2} = 2(T/(2\pi))^{3/2}$ is the scaled density of states. The diffusion matrix (D_{ij}) becomes

$$(D_{ij}) = \mu_0 \Gamma(2-\beta) n T^{1/2-\beta} \begin{pmatrix} 1 & (2-\beta)T \\ (2-\beta)T & (3-\beta)(2-\beta)T^2 \end{pmatrix}, \tag{16}$$

where μ_0 comes from the elastic scattering rate and Γ denotes the Gamma function with $\Gamma(\frac{1}{2}) = \sqrt{\pi}$ and $\Gamma(x+1) = x\Gamma(x)$ for $x > 0$. Typical choices for β are $\beta = \frac{1}{2}$, employed in [20], $\beta = 0$, used in [65], and $\beta = -\frac{1}{2}$, coming from the diffusion approximation of the hydrodynamic semiconductor model. Nonpolar phonon scattering may be modeled by

$\beta = \frac{1}{2}$ [64, Sec. 2.3.4], whereas $\beta = 0$ describes acoustic phonon scattering [10, formula (3.37)]. A computation shows that the current densities can be written as

$$J_n = \mu_0\Gamma(2-\beta)\big(\nabla(nT^{1/2-\beta}) - nT^{-1/2-\beta}\nabla V\big), \tag{17}$$

$$J_e = \mu_0\Gamma(3-\beta)\big(\nabla(nT^{3/2-\beta}) - nT^{1/2-\beta}\nabla V\big). \tag{18}$$

Finally, the inelastic collision integral W becomes (see [55] for details)

$$W = -\frac{3}{2}\frac{n(T-1)}{\tau_\beta(T)}, \quad \tau_\beta = \tau_{0,\beta}T^{1/2-\beta}, \tag{19}$$

where $\tau_{0,\beta} > 0$ is a constant depending on the elastic and inelastic scattering rates.

The remark that the assumptions needed to derive the explicit model can be weakened. Fermi-Dirac distribution functions have been considered in [57] and energy-transport models based on Fermi-Dirac statistics have been derived. Nonparabolic band structures in the sense of Kane $E(1+\alpha E) = \frac{1}{2}|k|^2$, where $\alpha > 0$ measures the nonparabolicity, lead to energy-transport models in which the energy integrals cannot be computed explicity [31, 56]. Simplifications are also obtained when assuming monotone spherically symmetric energy bands [10, 56].

3. Analytic results

3.1. **Existence and uniqueness of solutions.** The symmetric formulation (13)-(14) and the entropy estimate (15) are the key observations for the mathematical analysis of the energy-transport equations. In the following, we describe the main ideas and refer to [29] for the mathematical details.

We recall that the equations can be written as

$$\partial_t\rho_0(u) - \operatorname{div} J_0 = 0, \quad \partial_t\rho_1(u) - \operatorname{div} J_1 + J_0\cdot\nabla V = W(u), \tag{20}$$

where $\rho = (\rho_0,\rho_1) = (n, ne)$, $u = (u_0,u_1) = (\mu/T, -1/T)$, and the current densities are given by

$$J_i = D_{i0}(u)(\nabla u_0 + u_1\nabla V) + D_{i1}(u)\nabla u_1, \quad i = 0,1. \tag{21}$$

We assume that the electric potential is selfconsistently given by the Poisson equation

$$\lambda^2\Delta V = \rho_0(u) - C(x). \tag{22}$$

Equations (20)-(22) are solved in a bounded domain $\Omega \subset \mathbb{R}^d$ ($d \geq 1$) and complemented with the mixed Dirichlet-Neumann boundary conditions

$$u = u_D, \quad V = V_D \quad \text{on } \Gamma_D\times(0,\infty), \tag{23}$$

$$J_0\cdot\nu = J_1\cdot\nu = \nabla V\cdot\nu = 0 \quad \text{on } \Gamma_N\times(0,\infty), \tag{24}$$

where $\partial\Omega = \Gamma_D\cup\Gamma_N$ and ν denotes the exterior unit normal vector to $\partial\Omega$, and with the initial conditions

$$\rho(u(\cdot,0)) = \rho(u_I) \quad \text{in } \Omega. \tag{25}$$

In [29], the existence of weak solutions to (20)-(25) is shown under the following main assumptions. First, ρ is supposed to be a gradient and strongly monotone, i.e. there exist a

smooth scalar function χ and a number $\kappa_0 > 0$ such that $\rho = \nabla\chi$ and $(\rho(u)-\rho(\hat{u}))\cdot(u-\hat{u}) \geq \kappa_0|u-\hat{u}|^2$ for u, $\hat{u} \in \mathbb{R}^2$. Second, the diffusion matrix (D_{ij}) is symmetric and uniformly positive definite, i.e.

$$\sum_{i,j=0}^{1} D_{ij}(u)\xi_i\xi_j \geq \kappa_1|\xi|^2 \quad \text{for } \xi \in \mathbb{R}^2 \tag{26}$$

and for some constant $\kappa_1 > 0$. Third, the averaged scattering term W grows at most linearly and satisfies $(W(u)-W(\hat{u}))(u_1-\hat{u}_1) \leq 0$ for all u, $\hat{u} \in \mathbb{R}^2$. Finally, the temperature on the Dirichlet boundary has to be constant, $T_D = \text{const}$. These assumptions are rather restrictive. Indeed, for the explicit models derived in the previous section, the function $\rho(u) = (N_0(-u_1)^{-3/2}\exp(u_0), u_1)$ is monotone but generally not strongly monotone, and the diffusion matrix (16) is symmetric and positive definite but not uniformly positive definite (since n or T may vanish). Under the above hypotheses (and some regularity conditions for the initial and boundary data), for any terminal time $t_0 > 0$, there exists a weak solution (u, V) to (20)-(25) satisfying

$$u \in L^2(0,t_0;H^1(\Omega;\mathbb{R}^2)) \cap C^0([0,t_0];L^2(\Omega;\mathbb{R}^2)),$$
$$\rho(u) \in H^1(0,t_0;(H^1(\Omega;\mathbb{R}^2))^*) \cap L^2(0,t_0;L^2(\Omega;\mathbb{R}^2)), \quad V \in L^\infty(0,t_0;H^1(\Omega)).$$

The idea of the proof is to semi-discretize the equations by an implicit Euler scheme in t with grid size $\triangle t$ and to solve the semi-discrete system in the variables $w_0 = u_0 + u_1V$ and $w_1 = u_1$. Indeed, in these variables the system becomes [29]

$$\frac{1}{\triangle t}\big(b_0(w,V) - b_0(\overline{w},V)\big) - \operatorname{div}\widetilde{J}_0 = 0, \tag{27}$$

$$\frac{1}{\triangle t}\big(b_1(w,V) - b_1(\overline{w},V)\big) - \operatorname{div}\widetilde{J}_1 = W + \frac{1}{\triangle t}(V-\overline{V})b_0(w,V), \tag{28}$$

where $b_i(w,V) = \rho_i(u)$, w and V represent variables at time t and $\overline{w}$ and $\overline{V}$ variables at time $t - \triangle t$. The current densities are given by

$$\widetilde{J}_i = \sum_{j=0}^{1} L_{ij}(w,V)\nabla w_j, \quad i = 0,1, \tag{29}$$

where the new diffusion matrix (L_{ij}), defined in Section 2.3, is symmetric and positive definite. Then (27)-(29) is a system of nonlinear elliptic equations, which is solved by employing the Leray-Schauder fixed-point theorem. The key step is the compactness of the fixed-point operator which is obtained by means of the entropy estimates. For this, set $t_j = j\triangle t$ and denote the discrete solutions to (27)-(28) at step j by (w^j, V^j). It can be shown that the discrete entropy (or free energy)

$$S(u^j,V^j) = \int_\Omega \big(\rho(u)\cdot(u^j-u_D^j) - \chi(u^j) + \chi(u_D^j)\big)dx - \frac{u_{D,2}}{2}\int_\Omega |\nabla(V^j - V_D^j)|^2 dx,$$

where u_D^j and V_D^j is the boundary data evaluated at t_j, is uniformly bounded,

$$S(u^j,V^j)+\triangle t\sum_{k=0}^j\int_\Omega c_1^k\big(|\nabla w_0^k|^2+|\nabla w_1^k|^2\big)dx \\ +\triangle t c_2\sum_{k=0}^j|\nabla(V^k-V_D^k)|^2dx\le c_3,$$

where $c_1^k>0$ depends on κ_1 (see (26)) and the L^2 norm of u^k, and c_2, $c_3>0$ depend on the boundary data. Since ρ is assumed to be strongly monotone, this implies L^2 bounds for u^k and hence H^1 bounds for w^k and V^k. These bounds are sufficient for the fixed-point argument. In fact, the estimate also implies bounds independent of $\triangle t$, allowing for the limit $\triangle t\to 0$ in (27)-(29) using Aubin's lemma.

Uniqueness of solutions has been proved under the additional assumption that the diffusion coefficients D_{ij} depend on x only. More precisely, there is uniqueness of weak solutions in the class of functions satisfying $u\in L^\infty(0,t_0;W^{1,3/2}(\Omega))$ and $V\in L^\infty(0,t_0;W^{1,\infty}(\Omega))$ [54]. The proof is based on the so-called duality method.

The most restrictive conditions in the existence analysis are the *strong* monotonicity of ρ and the *uniform* positive definiteness of (D_{ij}). These conditions could be removed in [46, 21, 23] but only under other limiting assumptions. Griepentrog [46] proved the existence and uniqueness of stationary Hölder continuous weak solutions near the thermodynamic equilibrium using the implicit function theorem. A similar result has been shown in [37]. Stationary energy-transport equations which are defined on different domains have been examined in [44]. Near-equilibrium solutions to the time-dependent equations have been found in [21, 23].

3.2. **Weak sequential stability.** Weak sequential stability (in the sense of Feireisl [38]) means that, given a sequence of (smooth) solutions to a system of equations, there exists a subsequence which converges to a (weak) solution to this problem. Typically, the sequence of solutions solves an approximate system of equations, obtained from the original one by a Galerkin scheme or a semi-discretization in time, for instance, and the index of the sequence is related to the approximation parameter. Then weak stability implies that the limiting solution is a solution to the original system. In this section, we show the weak sequential stability for the energy-transport equations with $\beta=-1/2$ for vanishing electric fields and without the averaged scattering term W (see (8) and (17)-(18)):

$$\partial_t n=\Delta(nT),\quad \frac{3}{2}\partial_t(nT)=\frac{5}{2}\Delta(nT^2)\quad\text{in }\mathbb{T}^d,\ t>0, \tag{30}$$

$$n(\cdot,0)=n_I,\quad T(\cdot,0)=T_I\quad\text{in }\mathbb{T}^d, \tag{31}$$

where $\mathbb{T}^d$ is a d-dimensional torus (thus, imposing periodic boundary conditions). Here, we have rescaled the equations such that $\mu_0=1/\Gamma(5/2)$. These assumptions may be (at least partially) weakened, but they simplify the computations to follow. We assume that there exists a sequence $(n_\varepsilon,T_\varepsilon)$, $\varepsilon>0$, of positive smooth solutions to a (not specified)

approximation of (30)-(31). The lower bound for n_ε and T_ε may depend on the approximation parameter, $n_\varepsilon \geq c(\varepsilon) > 0$ and $T_\varepsilon \geq c(\varepsilon) > 0$ in $\mathbb{T}^d$. Our aim is to show that $(n_\varepsilon, T_\varepsilon)$ converges to a weak solution to (30)-(31). Although the construction of $(n_\varepsilon, T_\varepsilon)$ is an open problem, the weak sequential stability constitutes an important step in the global existence analysis of the energy-transport equations with physical transport coefficients.

We prove first some a priori estimates.

Lemma 1. *The following estimates hold:*

$$\frac{d}{dt}\int_{\mathbb{T}^d} n_\varepsilon \log(n_\varepsilon T_\varepsilon^{-3/2})dx + 4\int_{\mathbb{T}^d} |\nabla\sqrt{n_\varepsilon T_\varepsilon}|^2 dx \leq 0, \tag{32}$$

$$\frac{d}{dt}\int_{\mathbb{T}^d} n_\varepsilon^\alpha T_\varepsilon^\beta dx + c\int_{\mathbb{T}^d} |\nabla(n_\varepsilon^{\alpha/2} T_\varepsilon^{(\beta+1)/2})|^2 dx \leq 0, \tag{33}$$

where $(\alpha,\beta) = (3/2,-1)$, $(2,4)$, and $c > 0$ is some constant which depends on (α,β) but not on ε.

Proof. Employing $\log(n_\varepsilon T_\varepsilon^{-3/2})$ and $-3/(2T_\varepsilon)$ as test functions in (30), respectively, we obtain after some computations:

$$\begin{aligned}
\frac{d}{dt}\int_{\mathbb{T}^d} n_\varepsilon \log\Big(\frac{n_\varepsilon}{T_\varepsilon^{3/2}}\Big)dx &= \int_{\mathbb{T}^d}\left(\log\Big(\frac{n_\varepsilon}{T_\varepsilon^{3/2}}\Big)\partial_t n_\varepsilon - \frac{3}{2}\frac{1}{T_\varepsilon}\partial_t(n_\varepsilon T_\varepsilon)\right)dx \\
&= -\int_{\mathbb{T}^d} n_\varepsilon T_\varepsilon\left(\Big|\frac{\nabla n_\varepsilon}{n_\varepsilon}\Big|^2 + \frac{7}{2}\Big|\frac{\nabla T_\varepsilon}{T_\varepsilon}\Big|^2 + 2\frac{\nabla n_\varepsilon}{n_\varepsilon}\cdot\frac{\nabla T_\varepsilon}{T_\varepsilon}\right)dx \\
&\leq -\int_{\mathbb{T}^d} n_\varepsilon T_\varepsilon\Big|\frac{\nabla n_\varepsilon}{n_\varepsilon} + \frac{\nabla T_\varepsilon}{T_\varepsilon}\Big|^2 dx = -4\int_{\mathbb{T}^d}|\nabla\sqrt{n_\varepsilon T_\varepsilon}|^2 dx.
\end{aligned}$$

This proves the first inequality. For the second one, we calculate

$$\begin{aligned}
\frac{d}{dt}\int_{\mathbb{T}^d} n_\varepsilon^\alpha T_\varepsilon^\beta dx &= \int_{\mathbb{T}^d}\big((\alpha-\beta)n_\varepsilon^{\alpha-1}T_\varepsilon^\beta\partial_t n_\varepsilon + \beta n_\varepsilon^{\alpha-1}T_\varepsilon^{\beta-1}\partial_t(n_\varepsilon T_\varepsilon)\big)dx \\
&= -\int_{\mathbb{T}^d}\big(An_\varepsilon^{\alpha-2}T_\varepsilon^{\beta+1}|\nabla n_\varepsilon|^2 + 2Bn_\varepsilon^{\alpha-1}T_\varepsilon^\beta\nabla n_\varepsilon\cdot\nabla T_\varepsilon + Cn_\varepsilon^\alpha T_\varepsilon^{\beta-1}|\nabla T_\varepsilon|^2\big)dx,
\end{aligned}$$

where

$$\begin{aligned}
A &= \beta\Big(\frac{7}{3}\beta + \alpha - \frac{10}{3}\Big), \quad B = \frac{1}{2}\Big(\alpha(\alpha-1) + \frac{2}{3}\beta^2 - 4\beta + \frac{10}{3}\alpha\beta\Big), \\
C &= (\alpha-1)\Big(\alpha + \frac{2}{3}\beta\Big).
\end{aligned}$$

Now, we use the following result: If $A > 0$ and $AC - B^2 > 0$ then there exists $c_0 > 0$ such that $A|x|^2 + 2Bx\cdot y + C|y|^2 \geq c_0(|x|^2 + |y|^2)$ for all x, $y \in \mathbb{R}^d$. Thus, choosing $x = n_\varepsilon^{\alpha/2-1}T_\varepsilon^{(\beta+1)/2}\nabla n_\varepsilon$ and $y = n_\varepsilon^{\alpha/2}T_\varepsilon^{(\beta-1)/2}\nabla T_\varepsilon$, we infer that

$$\begin{aligned}
\frac{d}{dt}\int_{\mathbb{T}^d} n_\varepsilon^\alpha T_\varepsilon^\beta dx &\leq -c_0\int_{\mathbb{T}^d}\big(n_\varepsilon^{\alpha-2}T_\varepsilon^{\beta+1}|\nabla n_\varepsilon|^2 + n_\varepsilon^\alpha T_\varepsilon^{\beta-1}|\nabla T_\varepsilon|^2\big)dx \\
&\leq -c\int_{\mathbb{T}^d}|\nabla(n_\varepsilon^{\alpha/2}T_\varepsilon^{(\beta+1)/2})|^2 dx,
\end{aligned}$$

under the conditions that $A>0$ and $AC-B^2>0$. Since

$$AC-B^2 = -\frac{1}{4}\alpha^4 + \Big(-\frac{2}{3}\beta+\frac{1}{2}\Big)\alpha^3 - \frac{1}{9}\Big(\beta^2+6\beta+\frac{9}{4}\Big)\alpha^2 + \frac{4\beta}{9}\big(\beta^2+4\beta+3\big)\alpha - \frac{\beta^2}{9}\big(\beta^2+2\beta+16\big),$$

it is easy to verify that the pairs $(\alpha,\beta)=(3/2,-1)$, $(2,4)$ are admissible, finishing the proof. □

Notice that in the above proof, the approximate solutions have to be constructed in such a way that the corresponding test functions are admissible in the approximate scheme. For instance, this may be delicate when employing a Galerkin approximation.

Theorem 2. *Let $d\le 3$, $t_0>0$, and let $(n_\varepsilon,T_\varepsilon)$ be a sequence of positive smooth solutions to (possibly an approximate system of) (30)-(31). Then there exists a subsequence (which is not relabeled) such that $n_\varepsilon\to n$, $n_\varepsilon T_\varepsilon\to nT$ strongly in $L^2(0,t_0;L^2(\mathbb{T}^d))$, $n_\varepsilon T_\varepsilon^2\rightharpoonup nT^2$ weakly* in $L^\infty(0,t_0;L^2(\mathbb{T}^d))$, and (n,T) solves (30)-(31) in the sense of $L^2(0,t_0;H^{-2}(\mathbb{T}^d))$.*

Proof. We need to show that the estimates from Lemma 1 are sufficient to pass to the limit $\varepsilon\to 0$ in (30)-(31). First, since (30)-(31) conserve mass and energy, we have

$$\|n_\varepsilon\|_{L^\infty(0,t_0;L^1(\mathbb{T}^d))} + \|n_\varepsilon T_\varepsilon\|_{L^\infty(0,t_0;L^1(\mathbb{T}^d))} \le c, \tag{34}$$

where $c>0$ denotes here and in the following a constant independent of ε. Then, in view of (32),

$$\|\sqrt{n_\varepsilon T_\varepsilon}\|_{L^2(0,t_0;H^1(\mathbb{T}^d))}\le c.$$

Hence, since $(\sqrt{n_\varepsilon T_\varepsilon})$ is bounded in $L^\infty(0,t_0;L^2(\mathbb{T}^d))$ and in $L^2(0,t_0;L^6(\mathbb{T}^d))$ (because of the embedding $H^1(\mathbb{T}^d)\hookrightarrow L^6(\mathbb{T}^d)$ for $d\le 3$),

$$\nabla(n_\varepsilon T_\varepsilon) = 2\sqrt{n_\varepsilon T_\varepsilon}\nabla\sqrt{n_\varepsilon T_\varepsilon}$$

is bounded in $L^2(0,t_0;L^{3/2}(\mathbb{T}^d))$, and we obtain the bound

$$\|n_\varepsilon T_\varepsilon\|_{L^2(0,t_0;W^{1,3/2}(\mathbb{T}^d))}\le c. \tag{35}$$

Estimates for the time derivative $\partial_t(n_\varepsilon T_\varepsilon)$ follow from (33) with $\alpha=2$ and $\beta=4$. Indeed, this yields a bound for $(n_\varepsilon T_\varepsilon^2)$ in $L^\infty(0,t_0;L^2(\mathbb{T}^d))$ and therefore,

$$\|\partial_t(n_\varepsilon T_\varepsilon)\|_{L^\infty(0,t_0;H^{-2}(\mathbb{T}^d))}\le\frac{5}{3}\|n_\varepsilon T_\varepsilon^2\|_{L^\infty(0,t_0;L^2(\mathbb{T}^d))}\le c. \tag{36}$$

Next, we derive uniform bounds for n_ε. By (33) with $\alpha=3/2$ and $\beta=-1$, $(\nabla(n_\varepsilon^{3/4}))$ is bounded in $L^2(0,t_0;L^2(\mathbb{T}^d))$ and by (34), $(n_\varepsilon^{1/4})$ is bounded in $L^\infty(0,t_0;L^4(\mathbb{T}^d))$. Thus, $\nabla n_\varepsilon=(4/3)n_\varepsilon^{1/4}\nabla(n_\varepsilon^{3/4})$ is uniformly bounded in $L^2(0,t_0;L^{4/3}(\mathbb{T}^d))$. This implies that

$$\|n_\varepsilon\|_{L^2(0,t_0;W^{4/3}(\mathbb{T}^d))}\le c. \tag{37}$$

Furthermore, by (35),

$$\|\partial_t n_\varepsilon\|_{L^2(0,t_0;H^{-2}(\mathbb{T}^d))}\le\|n_\varepsilon T_\varepsilon\|_{L^2(0,T;L^2(\mathbb{T}^d))}\le c. \tag{38}$$

Now, in view of the estimates (35)-(36) and (37)-(38), we can employ Aubin's lemma, yielding the existence of subsequences of (n_ε) and $(n_\varepsilon T_\varepsilon)$ (which are not relabeled) such that, as $\varepsilon \to 0$,

$$n_\varepsilon \to n, \quad n_\varepsilon T_\varepsilon \to y \quad \text{strongly in } L^2(0,t_0;L^2(\mathbb{T}^d)). \tag{39}$$

Here we have used the compact embeddings $W^{1,4/3}(\mathbb{T}^d) \hookrightarrow L^2(\mathbb{T}^d)$ and $W^{1,3/2}(\mathbb{T}^d) \hookrightarrow L^2(\mathbb{T}^d)$ (if $d \le 3$). Since $(n_\varepsilon T_\varepsilon^2)$ is bounded in $L^\infty(0,t_0;L^2(\mathbb{T}^d))$, it holds (up to a subsequence)

$$n_\varepsilon T_\varepsilon^2 \rightharpoonup z \quad \text{weakly* in } L^\infty(0,t_0;L^2(\mathbb{T}^d)). \tag{40}$$

Moreover, again up to subsequences,

$$\partial_t n_\varepsilon \rightharpoonup \partial_t n, \quad \partial_t(n_\varepsilon T_\varepsilon) \rightharpoonup \partial_t y \quad \text{weakly in } L^2(0,t_0;H^{-2}(\mathbb{T}^d)).$$

We wish to identify y and z with expressions in n and T. First, we notice that the $L^\infty(0,t_0;L^2(\mathbb{T}^d))$ bound for $(n_\varepsilon T_\varepsilon^2)$ and the Fatou lemma give

$$\int_{\mathbb{T}^d} \liminf_{\varepsilon\to 0} \frac{(n_\varepsilon T_\varepsilon)^2}{n_\varepsilon} dx < \infty.$$

This shows that $y = 0$ in $\{n = 0\}$. We define $T := y/n$ if $n > 0$ and $T := 0$ if $n = 0$. Then $y = nT$. Furthermore, by (39) and (40),

$$(n_\varepsilon T_\varepsilon)^2 = n_\varepsilon \cdot n_\varepsilon T_\varepsilon^2 \rightharpoonup nz \quad \text{weakly in } L^2(0,t_0;L^1(\mathbb{T}^d)).$$

Hence, since $(n_\varepsilon T_\varepsilon)^2$ converges pointwise a.e. to $y^2 = (nT)^2$, we may identify $(nT)^2 = nz$ showing that $z = nT^2$ if $n > 0$ and also if $n = 0$ (since $T = 0$ if $n = 0$).

The above convergence results are sufficient to pass to the limit $\varepsilon \to 0$ yielding (30) in $L^2(0,t_0;H^{-2}(\mathbb{T}^d))$. The initial data is satisfied in the sense of $H^{-2}(\mathbb{T}^d)$. □

4. Numerical approximation

4.1. **Mixed finite-element approximation.** In this section, we describe two approaches to discretize the energy-transport equations by using mixed finite elements. The most important features of the mixed finite-element method are the current conservation (the current is introduced as an independent variable and continuity is directly imposed) and the ability to approximate accurately steep gradients.

The discretization devised in [31, 51, 52] is based on the "drift-diffusion" formulation (17)-(18) of the current equations, which allows for the use of well-understood discrete schemes developed originally for the semiconductor drift-diffusion equations. The stationary equations are written in the form

$$-\operatorname{div} J + \sigma g = f, \quad J = \nabla g - \frac{\nabla V}{T} g,$$

where J is either the particle or energy current density, $g = nT^{1/2-\beta}$ or $g = nT^{3/2-\beta}$, σg with $\sigma \ge 0$ is a zeroth-order term originating from the relaxation-time term (19), and f is some right-hand side. In [51], the equation is discretized in two space dimensions as follows.

First, the problem is written by means of a local Slotboom variable in a symmetric form, defining $y = \exp(-V/\overline{T})g$ in each element of the triangulation of the semiconductor domain, where $\overline{T}$ is some piecewise constant function approximating the electron temperature T. Then, the current density becomes $J = \exp(V/\overline{T})\nabla y$ in each element, which eliminates the drift term $g\nabla V/T$. This change of unknowns is also called exponential fitting.

In the second step, the symmetric form is discretized using mixed finite elements. For the case $\sigma = 0$ and constant temperature, a mixed scheme, based on the lowest-order Raviart-Thomas elements [70], has been introduced and discussed in [15] for $f = 0$ and in [14] for $f \neq 0$. The matrix associated with the scheme is an M-matrix if a weakly acute triangulation is used. This property guarantees a discrete maximum principle and, in particular, a nonnegative solution if the boundary data are nonnegative. Unfortunately, the M-matrix property does not hold anymore if $\sigma \neq 0$. In order to circumvent this fact we use the finite elements developed and analyzed by Marini and Pietra [66]. It has been proved that these elements provide an M-matrix for all $\sigma \geq 0$.

In the third step, a suitable discrete change of unknowns is performed to return to the original variable g. Finally, static condensation gives a nonlinear discrete system in the (discrete version of the) variable g only. The nonlinear problem is solved by a variant of the Gummel iteration procedure. The main idea is to solve the Poisson equation, in which the variable n is replaced by the local V-dependent Slotboom variable, by a Newton method, but to employ a fixed-point strategy for the remaining equations. It is well known that a Gummel-type iteration scheme is very sensitive to the choice of the initial guess, in particular far from thermal equilibrium. Therefore, the procedure is coupled with a continuation in the applied voltage. In [52], the two-dimensional mesh has been adaptively refined using an error estimator motivated by results of Hoppe and Wohlmuth.

The second numerical approach, employed in [41, 68], is based on the dual-entropy formulation (13)-(14). Compared to the previous approach, no convective terms appear, and the use of Raviart-Thomas-type mixed finite elements is sufficient to guarantee a monotone scheme. In [41], the three-dimensional stationary equations have been approximated using a hybridized mixed finite-element method with Raviart-Thomas-Nédélec elements. As above, static condensation allows for a reduction of the number of variables in the mixed-hybrid formulation. The resulting nonlinear algebraic system is solved by two iterative schemes, either using the full Newton method with a continuation in the applied voltage and a path-following algorithm or a Gummel-type strategy, which allows for a complete decoupling of the diffusion system such that only scalar equations have to be solved in each step. Since Gummel-type iteration procedures have a low convergence rate, a vector extrapolation technique was added to the algorithm to improve its convergence.

4.2. **Numerical simulations.** As a first numerical example, we simulate a two-dimensional MOSFET (metal-oxide semiconductor field-effect transistor) which can be employed as a voltage switch. It is the most used device in computer technology. The transistor has a size of $420\,\text{nm} \times 210\,\text{nm}$ with an effective channel (source to drain) length of 70 nm and an oxide thickness of 1.5 nm near the gate contact (see Figure 1). For the physical parameters, we refer to [52] from which the following pictures are taken. The transistor is simulated

using the energy-transport equations for electrons and the drift-diffusion equations for holes, discretized by the mixed Marini-Pietra finite-element scheme.

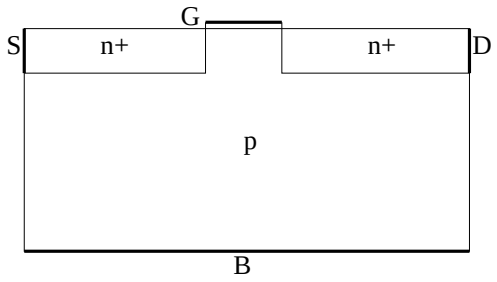

FIGURE 1. Geometry of the MOSFET with source S, drain D, gate G, and bulk B contacts.

The electron density and temperature are shown in Figure 2. Close to the gate contact in the channel region, the electron density is large compared to the bulk density. In this region, the electron temperature is high too. The temperature near the drain junction is larger than at the source junction since the electrons gain more energy from the electric field during their flow through the device.

As a second example we present some simulations for a three-dimensional gate-all-around MESFET (metal-semiconductor field-effect transistor). Compared to the device presented above, the gate contact is on all four sides of the transistor. This geometry allows for a very efficient switching behavior but its industrial production is more involved. The geometry of the device is shown in Figure 3. The channel length is $0.4\,\mu$m; the gate length is $0.33\,\mu$m. The transistor is simulated by employing the dual-entropy formulation of the energy-transport model, discretized by a mixed Raviart-Thomas-Nédélec finite-element scheme.

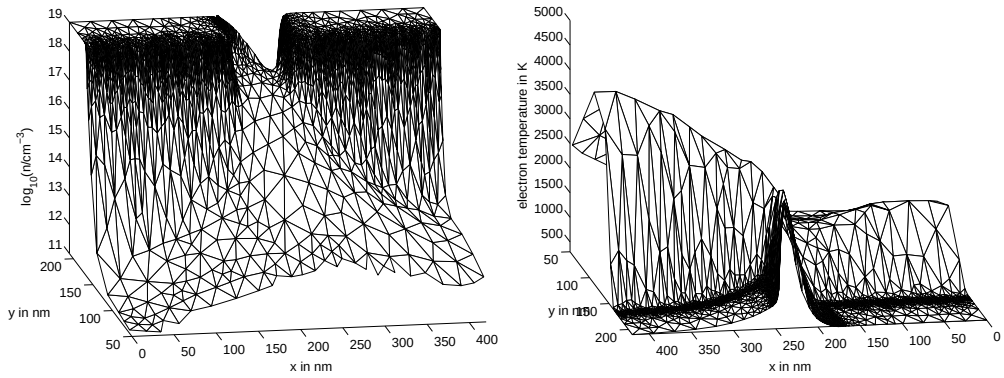

FIGURE 2. Electron density (left, gate contact at the back) and electron temperature (right, gate contact at the front) in a MOSFET with 70 nm channel length. A part of the bulk region is not shown.

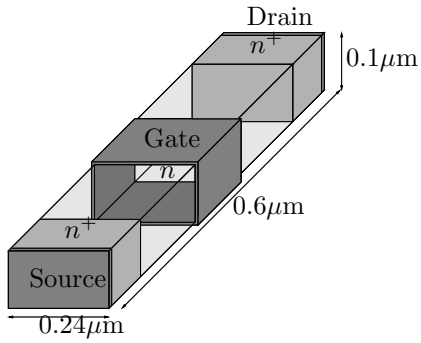

FIGURE 3. Geometry of the three-dimensional gate-all-around MESFET.

The particle density and electron temperature are depicted in Figure 4. The electron density is larger in the middle of the channel than close to the gate contacts since the transistor operates in the on-state. These electrons contribute to the temperature (and thermal energy) which is large at the end of the channel region.

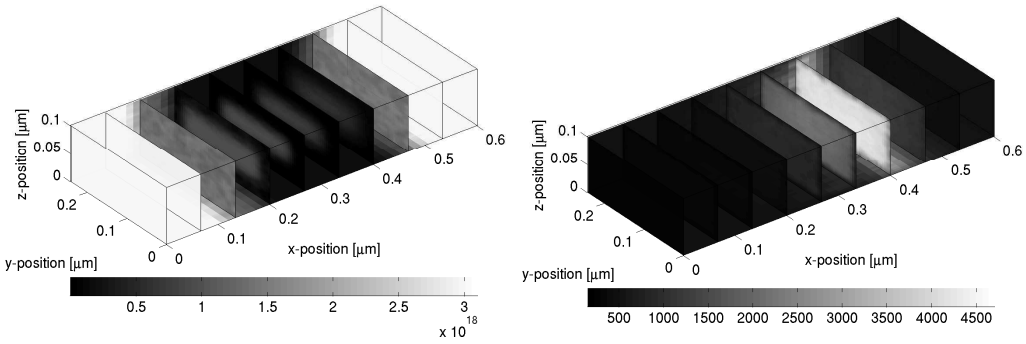

FIGURE 4. Electron density n in cm^{-3} (left) and electron temperature T in K (right) in the gate-all-around MESFET.

The current-voltage characteristics for the MESFET are presented in Figure 5 (left) at the gate. The current increases rapidly with the voltage and saturates for voltages larger than about 0.5 V. The saturation effect is much more pronounced than for the current-voltage characteristics from the drift-diffusion equations. The energy-transport current flow is smaller close to the gate contacts than in the middle of the channel due to the depletion region (Figure 5 right).

5. Further developments

5.1. **Energy-transport models including lattice heating.** Energy-transport equations model electron temperature effects but they neglect phenomena coming from the lattice heating. Nonisothermal models have been already introduced in the 1970s, employing drift-diffusion-type equations and heat flow models for the lattice temperature [1]. In

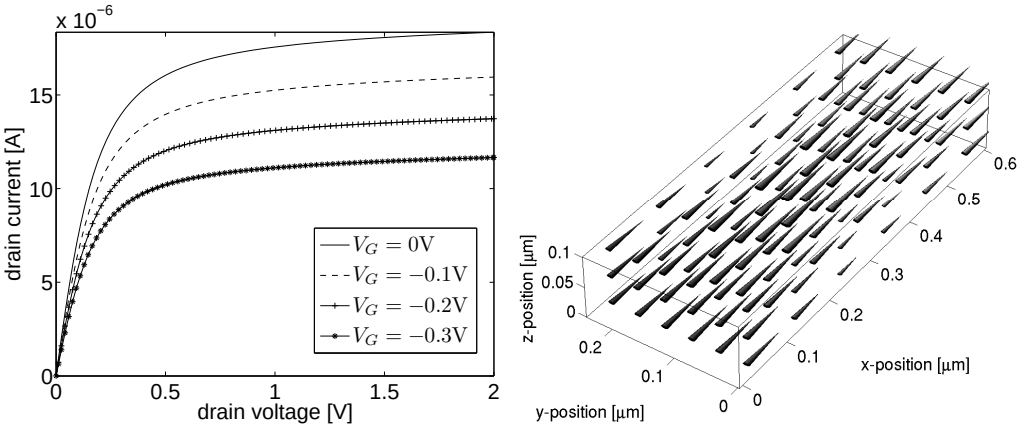

FIGURE 5. Current-voltage characteristics for various values of the gate voltage V_G (left) and electron current density in the gate-all-around MESFET (right).

[43, 76], a Joule heating term has been suggested as source term for the heat flow equation. More sophisticated but still heuristic source term models have been presented in [1, 28, 75]. Wachutka employed a thermodynamic approach to extend the drift-diffusion equations to the nonisothermal case [81]. Based on first principles of entropy maximization and partial local equilibrium, Albinus et al. [2] derived nonisothermal carrier transport equations and included also carrier temperatures. An energy-transport model taking into account the heat transfer between the devices and an electric circuit has been recently proposed in [3].

Models for different lattice and charge carrier temperatures have been developed in the 1990s. For instance, the unipolar hydrodynamic semiconductor equations have been coupled to a heat equation, with a coupling realized through the energy relaxation term [45, 61]. In [82], the heat equation and the energy-transport models for the carrier subsystems have been coupled. More recently, the energy-transport equations are coupled with a heat equation for the lattice temperature, a thermal network model (describing the heat evolution in interconnects, electric lines, etc.), and an electric circuit model (describing resistors, capacitors, and inductors, for instance) [16].

In [16], based on [9], the heat equation for the lattice temperature T_L is derived from thermodynamic principles, assuming that the total energy satisfies a standard balance equation. It turns out that T_L solves the heat equation

$$\rho\partial_t T_L - \operatorname{div}(\kappa_L \nabla T_L) = H,$$

where ρ is the product of the lattice material density and heat capacity, κ_L is the lattice heat conductivity, and the heat source term H is the sum of relaxation, recombination heat, band-energy Joule heating, and radiation effects (see [16] for details). This equation

is coupled to the energy-transport equations (8), where the current densities are given by

$$J_n = \nabla\big(\mu_n(T_L)T_L n\big) - \mu_n(T_L)T_L\frac{n}{T}\nabla V,$$
$$J_e = \frac{3}{2}\nabla\big(\mu_n(T_L)T_L nT\big) - \frac{3}{2}\mu_n(T_L)T_L n\nabla V,$$

and the electron mobility is defined by $\mu_n(T_L) = \mu_{n,0}(T_0/T_L)^\alpha$ with $\alpha > 0$.

It is well known in industrial applications that thermal effects in semiconductors are becoming stronger in smaller devices. This statement is verified in the following numerical simulations of one-dimensional ballistic diodes. A ballistic diode consists of a low-doped channel sandwiched between two highly doped contact regions. Figure 6 shows the effect of the lattice heating on the current-voltage characteristics of such a diode with two different channel sizes. It turns out that the influence of lattice heating is rather small for a 400 nm channel and becomes significant for very high applied bias only (Figure 6 left). For smaller devices, this influence becomes stronger even for rather small applied voltages (Figure 6 right). The same figure also presents the influence of the radiation of heat to the environment.

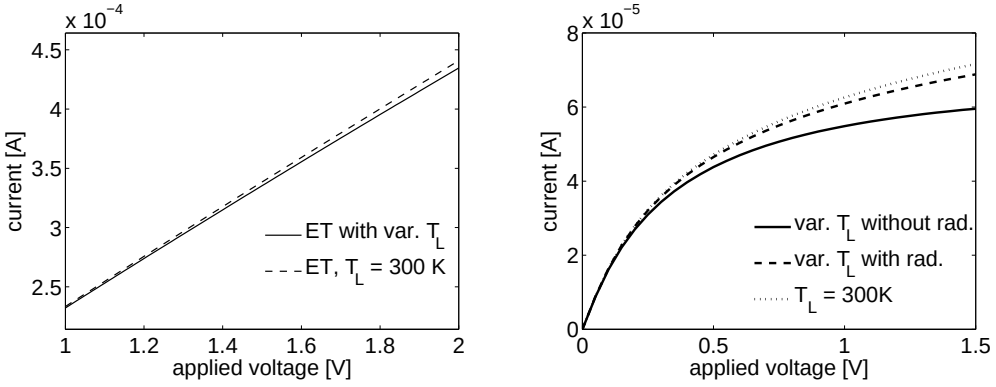

FIGURE 6. Current-voltage characteristics for ballistic diodes computed from the drift-diffusion model and the energy-transport (ET) model with constant and variable lattice temperature for the 400 nm channel (left) and 50 nm channel (right) device.

5.2. **Quantum energy-transport models.** The nanoscale structure of state-of-the-art semiconductor devices makes it necessary to incorporate quantum corrections in the existing simulation tools. In order to reduce the computational cost, one may devise fluid-type models incorporating quantum effects in an approximate way. One possibility is to employ macroscopic models derived from a Wigner-Boltzmann equation, such as the quantum hydrodynamic equations [42, 55] and the simpler quantum drift-diffusion equations [6, 60]. However, the former model is computationally quite involved, whereas the latter model does not account for temperature effects which seem to be important in quantum simulations [58]. Therefore, quantum energy-transport models may fulfill both demands of thermal modeling and computational efficiency.

Starting from a Wigner-Boltzmann equation with a relaxation-time collision term, a suitable Chapman-Enskog expansion leads to the balance equations of mass and energy (8) and the current relations [33]

$$J_n = \operatorname{div} P - n\nabla V, \quad J_e = \operatorname{div} U - (P + ne\mathbb{I})\nabla V + \frac{\varepsilon^2}{8} n\nabla\Delta V, \tag{41}$$

where ε is the scaled Planck constant, $\mathbb{I}$ the identity matrix in $\mathbb{R}^{d\times d}$, and P and U are the tensors

$$P = \int_{\mathbb{R}^d} p\otimes pM dk, \quad U = \frac{1}{2}\int_{\mathbb{R}^d} p\otimes p|p|^2 M dk,$$

Here, the matrix $p\otimes p$ has the components p_ip_j and the function M represents the quantum equilibrium, depending implicitly on the densities n and n [33, 55]. By expanding P and U in powers of ε^2, these tensors may be written in terms of n and ne and their derivatives. However, the mathematical (and thermodynamic) structure of the resulting equations is an open problem.

Another way to derive quantum-corrected energy-transport models is to perform a relaxation-time limit in the quantum hydrodynamic equations. Indeed, in the diffusive time and small velocity scaling, the following (simplifying) set of equations has been formally derived in [59]:

$$\partial_t n - \operatorname{div}\left(\nabla(nT) - n\nabla V - \frac{\varepsilon^2}{6} n\nabla\Big(\frac{\Delta\sqrt{n}}{\sqrt{n}}\Big)\right) = 0,$$
$$-\operatorname{div}(\kappa(n,T)\nabla T) = \frac{n}{\tau}(T_L - T),$$

where $\kappa(n,T)$ is the heat conductivity, T_L the (given) lattice temperature, and $\tau > 0$ the energy relaxation time. The first equation expresses mass conservation with a current density corresponding to (17) with $\beta = -1/2$, together with the quantum potential $\Delta\sqrt{n}/\sqrt{n}$, which is called the Bohm potential. For constant temperature, this equation reduces to the quantum drift-diffusion model. The second equation follows from the last equations in (8) and (41) in the small-velocity limit. An analysis of the above model has been performed in [59] for the case $\kappa(n,T) = n$.

Chen and Liu [25, 26] suggested a quantum-corrected energy-transport model, which lies in between the quantum drift-diffusion and energy-transport model. More specifically, the current density is given as in the quantum drift-diffusion case,

$$\partial_t n - \operatorname{div} J_n = 0, \quad J_n = \nabla(nT) - n\nabla V - \frac{\varepsilon^2}{6} n\nabla\Big(\frac{\Delta\sqrt{n}}{\sqrt{n}}\Big),$$

thus containing quantum effects, whereas the energy equation is written as

$$\partial_t(ne) - \operatorname{div} J_e + J_n\cdot\nabla V = W, \quad J_e = \frac{5}{2}J_nT + \kappa\nabla T.$$

Notice that this expression is consistent with the classical case, since, by (17) and (18) with $\beta=-1/2$,

$$J_e=\frac{5}{2}\big(\nabla(nT^2)-nT\nabla V\big)=\frac{5}{2}T\big(\nabla(nT)-n\nabla V\big)+\frac{5}{2}nT\nabla T,$$

which corresponds to the above expression with $\kappa=(5/2)nT$ (and $\varepsilon=0$). The numerical simulations in [25] for a MOS device show that the current density of the quantum-corrected model is smaller than that of the classical energy-transport model.

5.3. **Optimal doping profiles and energy-transport models.** The functionality of semiconductor devices may be improved by methods from mathematical optimization. A major objective in optimal design is to improve the current flow over the contacts by modifying the doping profile. The doping concentration then enters as a source term in the semiconductor model and plays the role of the design variable. First approaches have been based on black-box optimization tools or nonlinear least-square methods [63, 78]. The disadvantage of this approach is the large computational cost. More recently, the optimization problem has been solved in the framework of optimal control of the drift-diffusion equations, which makes possible the design of fast algorithms [17, 50].

Energy-transport models have been included in the optimal control approach in [35] and the first-order optimality system has been derived. Numerical results have been presented in [36] for the energy-transport system in the dual-entropy formulation (13)-(14). The design objective is to adjust the current $\widetilde{J}_n$ at some Ohmic constant Γ by changing the reference doping profile $C_{\rm ref}$. At the contact Γ, we prescribe the desired current I_d. Then the aim is to minimize the cost functional

$$F(w,V,C)=\frac{1}{2}\left|\int_{\Gamma_0}\widetilde{J}_n(w,V)\cdot\nu ds-I_g\right|+\frac{\gamma}{2}\int_\Omega|\nabla(C-C_{\rm ref})|^2dx,$$

where ν denotes the exterior unit normal to $\partial\Omega$, under the constraint that (w,V) solves the stationary energy-transport system (13)-(14) with mixed Dirichlet-Neumann boundary conditions. The parameter $\gamma>0$ allows one to balance the effective cost. The solvability of this constrained optimization problem has been proved in [35].

Acknowledgements

The author acknowledges partial support from the Austrian Science Fund (FWF), grant P20214 and WK "Differential Equations", the German Science Foundation (DFG), grant JU 359/7, and the Austrian-Croatian Project of the Austrian Exchange Service (ÖAD) and the Ministry of Science, Education, and Sports of the Republic of Croatia (MZOS).

References

[1] M. Adler. Accurate calculations of the forward drop and power dissipation in thyristors. *IEEE Trans. Electr. Dev.* 25 (1978), 16-22.

[2] G. Albinus, H. Gajewski, and R. Hünlich. Thermodynamic design of energy models of semiconductor devices. *Nonlinearity* 15 (2002), 367-383.

[3] G. Alì and M. Carini. Energy-transport models for semiconductor devices and their coupling with electric networks. In: V. Cutello, G. Fotia, and L. Puccio (eds.), *Applied and Industrial Mathematics in Italy II. Selected Contributions from the 8th SIAMI Conference*, Ser. Adv. Math. Appl. Sci. 72, pp. 13-24. World Scientific, Singapore, 2008.
[4] G. Alì and I. Torcicollo. Nonlinear stability of smooth solutions of the energy-transport model for semiconductors. *Z. Angew. Math. Mech.* 85 (2005), 267-276.
[5] W. Allegretto and H. Xie. Nonisothermal semiconductor systems. In: *Comparison Methods and Stability Theory* (Waterloo, ON, 1993), Lect. Notes Pure Appl. Math. 162, pp. 17-24. Dekker, New York, 1994.
[6] M. Ancona. Diffusion-drift modeling of strong inversion layers. *COMPEL* 6 (1987), 11-18.
[7] Y. Apanovich, E. Lyumkis, B. Polski, A. Shur, and P. Blakey. A comparison of energy balance and simplified hydrodynamic models for GaAs simulation. *COMPEL* 12 (1993), 221-230.
[8] N. Ashcroft and N. Mermin. *Solid State Physics.* Sanners College, Philadelphia, 1976.
[9] U. Bandelow, H. Gajewski, and R. Hünlich. Fabry-Perot lasers: thermodynamic-based modeling. In: J. Piprek (ed.), *Optoelectronic Devices. Advanced Simulation and Analysis*, pp. 63–85. Springer, Berlin, 2005.
[10] N. Ben Abdallah and P. Degond. On a hierarchy of macroscopic models for semiconductors. *J. Math. Phys.* 37 (1996), 3308-3333.
[11] N. Ben Abdallah, P. Degond, and S. Génieys. An energy-transport model for semiconductors derived from the Boltzmann equation. *J. Stat. Phys.* 84 (1996), 205-231.
[12] F. Bosisio, R. Sacco, F. Saleri, and E. Gatti. Exponentially fitted mixed finite volumes for energy balance models in semiconductor device simulation. In: H. Bock et al. (eds.), *Proceedings of ENUMATH 97*, pp. 188-197. World Scientific, Singapore, 1998.
[13] K. Brennan. *The Physics of Semiconductors.* Cambridge University Press, Cambridge, 1999.
[14] F. Brezzi, L. Marini, and P. Pietra. Numerical simulation of semiconductor devices. *Comput. Methods Appl. Mech. Engrg.* 75 (1989), 493-514.
[15] F. Brezzi, L. Marini, and P. Pietra. Two-dimensional exponential fitting and applications to drift-diffusion models. *SIAM J. Numer. Anal.* 26 (1989), 1342-1355.
[16] M. Brunk and A. Jüngel. Self-heating in a coupled thermo-electric circuit-device model. Submitted for publication, 2009.
[17] M. Burger and R. Pinnau. Fast optimal design for semiconductor devices. *SIAM J. Appl. Math.* 64 (2003), 108-126.
[18] C. Chainais-Hillairet. Discrete duality finite volume schemes for two-dimensional drift-diffusion and energy-transport models. *Int. J. Numer. Meth. Fluids* 59 (2009), 239-257.
[19] C. Chainais-Hillairet and Y.-J. Peng. Finite volume scheme for semiconductor energy-transport model. In: *Elliptic and Parabolic Problems*, Progr. Nonlin. Diff. Eqs. Appl. 63, pp. 139-146. Birkhäuser, Basel, 2005.
[20] D. Chen, E. Kan, U. Ravaioli, C. Shu, and R. Dutton. An improved energy transport model including nonparabolicity and non-Maxwellian distribution effects. *IEEE Electr. Device Letters* 13 (1992), 26-28.
[21] L. Chen and L. Hsiao. The solution of Lyumkis energy transport model in semiconductor science. *Math. Meth. Appl. Sci.* 26 (2003), 1421-1433.
[22] L. Chen, L. Hsiao, and Y. Li. Global existence and asymptotic behavior to the solutions of 1-D Lyumkis energy transport model for semiconductors. *Quart. Appl. Math.* 62 (2004), 337-358.
[23] L. Chen, L. Hsiao, and Y. Li. Large time behavior and energy relaxation time limit of the solutions to an energy transport model in semiconductors. *J. Math. Anal. Appl.* 312 (2005), 596-619.
[24] R.-C. Chen and J.-L. Liu. An iterative method for adaptive finite element solutions of an energy transport model of semiconductor devices. *J. Comput. Phys.* 189 (2003), 579-606.
[25] R.-C. Chen and J.-L. Liu. A quantum corrected energy-transport model for nanoscale semiconductor devices. *J. Comput. Phys.* 204 (2005), 131-156.

[26] R.-C. Chen and J.-L. Liu. An accelerated monotone iterative method for the quantum-corrected energy transport model. *J. Comput. Phys.* 227 (2008), 6226-6240.
[27] I. Choquet, P. Degond, and C. Schmeiser. Energy-transport models for charge carriers involving impact ionization in semiconductors. *Transp. Theory Stat. Phys.* 32 (2003), 99-132.
[28] A. Chryssafis and W. Love. A computer-aided analysis of one-dimensional thermal transients in n-p-n power transistors. *Solid-State Electr.* 22 (1979), 249-256.
[29] P. Degond, S. Génieys, and A. Jüngel. A system of parabolic equations in nonequilibrium thermodynamics including thermal and electrical effects. *J. Math. Pures Appl.* 76 (1997), 991-1015.
[30] P. Degond, S. Génieys, and A. Jüngel. A steady-state system in nonequilibrium thermodynamics including thermal and electrical effects. *Math. Meth. Appl. Sci.* 21 (1998), 1399-1413.
[31] P. Degond, A. Jüngel, and P. Pietra. Numerical discretization of energy-transport models for semiconductors with nonparabolic band structure. *SIAM J. Sci. Comput.* 22 (2000), 986-1007.
[32] P. Degond, C. Levermore, and C. Schmeiser. A note on the energy-transport limit of the semiconductor Boltzmann equation. In: N. Ben Abdallah et al. (eds.), *Proceedings of Transport in Transition Regimes* (Minneapolis, 2000), IMA Math. Appl. 135, pp. 137-153. Springer, New York, 2004.
[33] P. Degond, F. Méhats, and C. Ringhofer. Quantum energy-transport and drift-diffusion models. *J. Stat. Phys.* 118 (2005), 625-665.
[34] P. Degond and B. Wennberg. Mass and energy balance laws derived from high-field limits of thermostatted Boltzmann equations. *Commun. Math. Sci.* 5 (2007), 355-382.
[35] C. Drago and A. Anile. An optimal control approach for an energy transport model in semiconductor design. In: *Proceedings SCEE 2004*. Mathematics in Industry 9, pp. 323-330. Springer, Berlin, 2006.
[36] C. Drago and R. Pinnau. Optimal dopant profiling based on energy-transport semiconductor models. *Math. Models Meth. Appl. Sci.* 18 (2008), 195-214.
[37] W. Fang and K. Ito. Existence of stationary solutions to an energy drift-diffusion model for semiconductor devices. *Math. Models Meth. Appl. Sci.* 11 (2001), 827-840.
[38] E. Feireisl. *Dynamics of Viscous Compressible Fluids*. Oxford University Press, Oxford, 2004.
[39] A. Forghieri, R. Guerrieri, P. Ciampolini, A. Gnudi, M. Rudan, and G. Baccarani. A new discretization strategy of the semiconductor equations comprising momentum and energy balance. *IEEE Trans. Computer-Aided Design Integr. Circuits Sys.* 7 (1988), 231-242.
[40] M. Fournié. Numerical discretization of energy-transport model for semiconductors using high-order compact schemes. *Appl. Math. Letters* 15 (2002), 727-734.
[41] S. Gadau and A. Jüngel. A three-dimensional mixed finite-element approximation of the semiconductor energy-transport equations. *SIAM J. Sci. Comput.* 31 (2008), 1120-1140.
[42] C. Gardner. The quantum hydrodynamic model for semiconductor devices. *SIAM J. Appl. Math.* 54 (1994), 409-427.
[43] S. Gaur and D. Navon. Two-dimensional carrier flow in a transistor structure under nonisothermal conditions. *IEEE Trans. Electr. Dev.* 23 (1976), 50-57.
[44] A. Glitzky and R. Hünlich. Stationary solutions to an energy model for semiconductor devices where the equations are defined on different domains. *Math. Nachr.* 281 (2008), 1676-1693.
[45] T. Grasser. *Mixed-Mode Device Simulation*. Ph.D. Thesis, Vienna University of Technology, Austria, 1999.
[46] J. Griepentrog. An application of the implicit function theorem to an energy model of the semiconductor theory. *Z. Angew. Math. Mech.* 79 (1999), 43-51.
[47] S. de Groot and P. Mazur. *Nonequilibrium Thermodynamics*. Dover Publications, New York, 1984.
[48] P. Guan and B. Wu. Existence of weak solutions to a degenerate time-dependent semiconductor equations with temperature effect. *J. Math. Anal. Appl.* 332 (2007), 367-380.
[49] W. Hänsch and M. Miura-Mattausch. The hot-electron problem in small semiconductor devices. *J. Appl. Phys.* 60 (1986), 650-656.
[50] M. Hinze and R. Pinnau. An optimal control approach to semiconductor design. *Math. Models Meth. Appl. Sci.* 12 (2002), 89-107.

[51] S. Holst, A. Jüngel, and P. Pietra. A mixed finite-element discretization of the energy-transport equations for semiconductors. *SIAM J. Sci. Comput.* 24 (2003), 2058-2075.
[52] S. Holst, A. Jüngel, and P. Pietra. An adaptive mixed scheme for energy-transport simulations of field-effect transistors. *SIAM J. Sci. Comput.* 25 (2004), 1698-1716.
[53] J. Jerome and C.-W. Shu. Energy models for one-carrier transport in semiconductor devices. In: W. Coughran et al. (eds.), *Semiconductors*, Part II, IMA Math. Appl. 59, pp. 185-207. Springer, New York, 1994.
[54] A. Jüngel. Regularity and uniqueness of solutions to a parabolic system in nonequilibrium thermodynamics. *Nonlin. Anal.* 41 (2000), 669-688.
[55] A. Jüngel. *Transport Equations for Semiconductors.* Lect. Notes Phys. 773. Springer, Berlin, 2009.
[56] A. Jüngel, S. Krause, and P. Pietra. A hierarchy of diffusive higher-order moment equations for semiconductors. *SIAM J. Appl. Math.* 68 (2007), 171-198.
[57] A. Jüngel, S. Krause, and P. Pietra. Diffusive semiconductor moment equations using Fermi-Dirac statistics. Submitted for publication, 2009.
[58] A. Jüngel and J.-P. Milišić. Physical and numerical viscosity for quantum hydrodynamics. *Commun. Math. Sci.* 5 (2007), 447-471.
[59] A. Jüngel and J.-P. Milišić. A simplified quantum energy-transport model for semiconductors. Work in progress, 2009.
[60] A. Jüngel and R. Pinnau. A positivity-preserving numerical scheme for a nonlinear fourth order parabolic equation. *SIAM J. Numer. Anal.* 39 (2001), 385-406.
[61] M. Knaipp. *Modellierung von Temperatureinflüssen in Halbleiterbauelementen.* Ph.D. Thesis, Vienna University of Technology, Austria, 1998.
[62] C. Lab and P. Caussignac. An energy-transport model for semiconductor heterostructure devices: Application to AlGaAs/GaAs MODFETs. *COMPEL* 18 (1999), 61-76.
[63] W. Lee, S. Wang, and K. Teo. An optimization approach to a finite dimensional parameter estimation problem in semiconductor device design. *J. Comput. Phys.* 156 (1999), 241-256.
[64] M. Lundstrom. *Fundamentals of Carrier Transport.* 2nd edition, Cambridge University Press, Cambridge, 2000.
[65] E. Lyumkis, B. Polsky, A. Shur, and P. Visocky. Transient semiconductor device simulation including energy balance equation. *COMPEL* 11 (1992), 311-325.
[66] L. D. Marini and P. Pietra. New mixed finite element schemes for current continuity equations. *COMPEL* 9 (1990), 257-268.
[67] P. Markowich, C. Ringhofer, and C. Schmeiser. *Semiconductor Equations.* Springer, Vienna, 1990.
[68] A. Marrocco and P. Montarnal. Simulation de modèles "energy transport" à l'aide des éléments finis mixtes. *C. R. Acad. Sci. Paris, Sér. I* 323 (1996), 535-541.
[69] R. Melnik and H. He. Modelling nonlocal processes in semiconductor devices with exponential difference schemes. *J. Engrg. Math.* 38 (2000), 233-263.
[70] P. Raviart and J. Thomas. A mixed finite element method for second order elliptic equations. In: *Mathematical Aspects of the Finite Element Method* (Proc. Conf. Rome 1975), *Lecture Notes in Math.* 606, 292-315. Springer, New York, 1977.
[71] C. Ringhofer. An entropy-based finite difference method for the energy transport system. *Math. Models Meth. Appl. Sci.* 11 (2001), 769-796.
[72] V. Romano. 2D numerical simulation of the MEP energy-transport model with a finite difference scheme. *J. Comput. Phys.* 221 (2007), 439-468.
[73] M. Rudan, A. Gnudi, and W. Quade. A generalized approach to the hydrodynamic model of semiconductor equations. In: G. Baccarani (ed.), *Process and Device Modeling for Microelectronics*, 109-154. Elsevier, Amsterdam, 1993.
[74] M. Rudan, M. Vecchi, and D. Ventura. The hydrodynamic model in semiconductors – coeffcient calculation for the conduction band of silicon. In: P. Marcati, P. Markowich, and R. Natalini (eds.), *Mathematical Problems in Semiconductors*, pp. 186-214. Pitman Res. Notes, Longman, Essex, 1995.

[75] S. Selberherr. *Analysis and Simulation of Semiconductor Devices*. Springer, Vienna, 1984.
[76] D. Sharma and K. Ramanathan. Modeling thermal effects on MOS I-V characteristics. *IEEE Electr. Dev. Lett.* EDL-4 (1983), 362-364.
[77] K. Souissi, F. Odeh, H. Tang, and A. Gnudi. Comparative studies of hydrodynamic and energy transport models. *COMPEL* 13 (1994), 439-453.
[78] M. Stockinger, R. Strasser, R. Plasun, A. Wild, and S. Selberherr. A qualitative study on optimized MOSFET doping profiles. In: *Proceedings SISPAD 98 Conference*, pp. 77-80, 1998.
[79] R. Stratton. Diffusion of hot and cold electrons in semiconductor barriers. *Phys. Rev.* 126 (1962), 2002-2014.
[80] S.-Q. Tang and D.-P. Zhang. Pseudo-hydrodynamic approximation for transient computation of energy-transport models in semiconductors. *Chin. Phys. Lett.* 22 (2005), 2633-2636.
[81] G. Wachutka. Rigorous thermodynamic treatment of heat generation and conduction in semiconductor device modeling. *IEEE Trans. Comp. Aided Design* 9 (1990), 1141-1149.
[82] G. Wachutka. *Consistent treatment of carrier emission and capture kinetices in electrothermal and energy transport models*. Microelectr. J. 26 (1995), 307-315.
[83] D. Woolard, H. Tian, R. Trew, M. Littlejohn, and K. Kim. Hydrodynamic electron-transport: Non-parabolic corrections to the streaming terms. *Phys. Rev. B* 44 (1991), 11119-11132.
[84] H.-M. Yin. The semiconductor system with temperature effect. *J. Math. Anal. Appl.* 196 (1995), 135-152.

Institute for Analysis and Scientific Computing, Vienna University of Technology, Wiedner Hauptstr. 8-10, 1040 Wien, Austria
E-mail address: juengel@anum.tuwien.ac.at